Analysis of thermoelastic effects accompanying the deformation of PMMA and PC polymers

Stéphane Moreau, Andre Chrysochoos, Jean Michel Muracciole, Bertrand Wattrisse

Analysis of thermoelastic effects accompanying the deformation of PMMA and PC polymers
Analyse des effets thermoélastiques accompagnant la déformation du PMMA et du PC

S. Moreau, A. Chrysochoos, J.-M. Muracciole, B. Wattrisse
Laboratoire de Mécanique et Génie Civil, UMR5508 UMII-CNRS, Place E.Bataillon, CC048, 34095 Montpellier cedex 05, France
Tel.: +33 (0) 467 143 432
Fax: +33 (0) 467 144 792
E-mail: smoreau@lmgc.univ-montp2.fr

Abstract:

A thermographic analysis of heat sources accompanying the deformation of PMMA and PC polymers revealed several possible ways of introducing the thermoelastic coupling effects in the modelling. Therefore we used two basic linear viscoelastic models in which an elastic component was replaced by a thermoelastic branch. This *Note* highlights the practical interest of our approach for describing variations in thermoelastic sources during pulsating tensile testing of PMMA and PC samples.
Polymers /PMMA /PC /IR thermography /thermoelasticity

Résumé:

L'analyse thermographique des sources de chaleur accompagnant la déformation des polymères PMMA et PC nous a conduit à introduire de plusieurs façons possibles les effets de couplage thermoélastique dans la modélisation. Pour cela, nous avons utilisé deux modèles viscoélastiques linéaires élémentaires dans lesquels un composant élastique a été remplacé par une branche thermoélastique. La *Note* montre l'intérêt pratique d'une telle approche pour décrire l'évolution des sources thermoélastiques du PMMA et du PC lors d'essais de traction ondulée.
Polymères /PMMA /PC /thermographie IR /thermoélasticité

1. Introduction

Within the framework of "small perturbations", polymers are generally considered as viscoelastic materials. The linear theory of viscoelasticity shows that any model is a particular case of Biot's general model [1], and consequently any "series" model (Poynting-Thomson type (PT)) having N relaxation times is mechanically equivalent to a "parallel" model (Zener type (Z)) [2-3]. From a thermodynamic standpoint, it is also interesting to note that two equivalent models dissipate the same amount of mechanical energy.

However, recent experimental studies on the mechanical and energy behaviour of several polymers led us to consider linear viscothermoelastic models instead of viscoelastic models [4]. In order to draw up a complete energy balance associated with the deformation process, infrared imaging techniques have been used [5] to estimate the intensity and distribution of heat sources developed during uniaxial pulsating tests with increasing stress amplitude. An analysis of the mechanical and calorimetric effects then showed that for small deformations ($<2.10^{-2}$) and low strain rates ($<5.10^{-4}$ s^{-1}), *i.e.* low stress levels (<50 MPa), the intensity of dissipation d_1 remained low compared to the thermoelastic source amplitude Δs_{the} ($d_1 \approx \Delta s_{the}$ /30). Moreover, the experiments showed that the thermoelastic effects could vary between polymers under the same testing conditions. The thermoelastic effects were introduced into two PT and Z type models in order to take these results into account.

This *Note* first indicates how these models may give different thermoelastic responses under the same loading conditions. Then, based on a thermographic analysis of calorimetric effects, the thermoelastic sources induced by the deformation of PMMA and PC polymers are shown to be respectively in a quite good agreement with predictions generated by PT and Z type models.

2. PT and Z type models taking thermoelasticity into account

We considered one-dimensional PT and Z type rheological models with thermoelastic branches replacing the elastic springs. For simplicity, the spectrum of each model was limited to only one relaxation time. All configurations were naturally considered in [4]. Here, we have eliminated those that give the same thermoelastic responses under the same loading conditions and those for which the dilatation parameters are not separately measurable using standard dilatometry techniques. The two remaining candidate models are plotted in Figure 1.

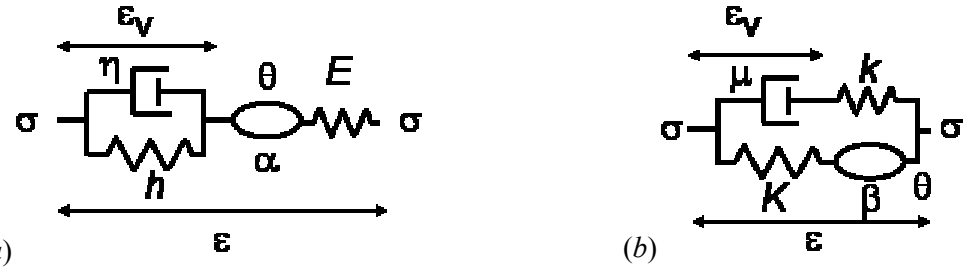

Figure 1: Basic sketch of 1D thermoviscoelastic models: (*a*) PT type**;** (*b*) Z type
Figure 1: Schématisation des modèles thermoviscoélastiques 1D de (a) PT et (b) Z.

For small perturbations, the state variables chosen for both models are: $\theta = T - T_0$ the temperature variation with respect to the room temperature (named T_0), ε the tensile strain and ε_v the viscous part of ε. Our experimental observations indicated that the temperature variations remained low, so $\theta << T_0$. The E, h, K, k constants are elasticity moduli, α and β are linear thermal expansion coefficients, and η and μ are viscosity parameters. The material constants ρ, C and κ, representing the density, the specific heat and the isotropic conduction coefficient, respectively, are still introduced. Both models belong to the classical framework of generalized standard models [6], so derivation of the heat equation then enabled us to specify the form taken by the different heat sources.

2.1. PT type model

With the above notations, the volume free energy and the dissipation potential are as follows:

$$\begin{cases} \psi^{\mathrm{PT}}(\theta,\varepsilon,\varepsilon_v) = \dfrac{E}{2}(\varepsilon - \alpha\theta - \varepsilon_v)^2 - \left(\dfrac{E\alpha^2}{2} + \dfrac{\rho_0 C_0}{2T_0}\right)\theta^2 - s_0\theta + \dfrac{h}{2}\varepsilon_v^2 \\ \varphi^{\mathrm{PT}}(q,\dot{\varepsilon},\dot{\varepsilon}_v) = \dfrac{q.q}{2\kappa T_0} + \dfrac{\eta}{2}\dot{\varepsilon}_v^2 \end{cases}, \tag{1}$$

where s_0 is the specific entropy associated with the initial state $(\theta, \varepsilon, \varepsilon_v)=(0, 0, 0)$, and where q is the heat influx vector. The heat diffusion equation can then be written as:

$$\rho C\dot{\theta} + \mathrm{div}q = \eta\dot{\varepsilon}_v^2 - E\alpha T_0(\dot{\varepsilon} - \dot{\varepsilon}_v), \tag{2}$$

where the intrinsic dissipation $d_1^{\mathrm{PT}} = \eta\dot{\varepsilon}_v^2$ and the thermoelastic source $s_{\mathrm{the}}^{\mathrm{PT}} = -E\alpha T_0(\dot{\varepsilon} - \dot{\varepsilon}_v)$. Equation (2) is classically derived by combining the local expression of the two principles of thermodynamics [7] in the particular case of potentials defined by equation (1). Since the dissipation potential does not depend on $\dot{\varepsilon}$, the stress is, by construction, written as:

$$\sigma = \psi_{,\varepsilon}^{PT} = E\left(\varepsilon - \alpha\theta - \varepsilon_v\right). \tag{3}$$

This equation allowed us to draw up experimental protocols to estimate the two parameters α and E. α was estimated by using dilatometry tests performed at very slow ramp heating so that the stress and viscous strain remained at zero:

$$\left.\frac{d\varepsilon}{d\theta}\right]_{\sigma=0,\varepsilon_v=0} = \alpha. \tag{4}$$

We stress that to be able to interpret the structural data given by a dilatometer in terms of material characteristics, the temperature rate must be sufficiently low to ensure a suitable thermal equilibrium throughout the sample. This constraint eliminates the possibility of distinguishing instantaneous from delayed dilatation mechanisms.

In a second step, we estimated the elasticity modulus E by considering the initial slope of a stress-strain curve corresponding to adiabatic loading performed at a sufficiently high strain rate. By neglecting the viscous strain, the intrinsic dissipation and the heat losses by conduction, equations (2) and (3) then give:

$$\left.\frac{d\sigma}{d\varepsilon}\right]_{\varepsilon_v=0,\,q=0} = E\left(1 + \frac{E\alpha^2 T_0}{\rho C}\right). \tag{5}$$

2.2. Z type model

The volume free energy and the dissipation potential associated with the Z type model are as follows:

$$\begin{cases} \psi^Z(\theta,\varepsilon,\varepsilon_v) = \dfrac{K}{2}\left(\varepsilon - \beta\theta\right)^2 - \left(\dfrac{K\beta^2}{2} + \dfrac{\rho_0 C_0}{2T_0}\right)\theta^2 - s_0\theta + \dfrac{k}{2}\left(\varepsilon - \varepsilon_v\right)^2 \\ \varphi^Z(q,\dot{\varepsilon},\dot{\varepsilon}_v) = \dfrac{q.q}{2\kappa T_0} + \dfrac{\mu}{2}\dot{\varepsilon}_v^2 \end{cases}, \tag{6}$$

where s_0 and q have the same meaning as in the previous model. The corresponding heat equation is written as:

$$\rho C\dot{\theta} + \mathrm{div}q = \mu\dot{\varepsilon}_v^2 - K\beta T_0\dot{\varepsilon}. \tag{7}$$

In the right-hand member of equation (7), the intrinsic dissipation d_1^Z is $\mu\dot{\varepsilon}_v^2$ while the thermoelastic coupling source s_{the}^Z corresponds to $-K\beta T_0\dot{\varepsilon}$. With the irreversible part of the stress being zero, the stress is derived from the state equation:

$$\sigma = \psi_{,\varepsilon}^Z = K\left(\varepsilon - \beta\theta\right) + k\left(\varepsilon - \varepsilon_v\right). \tag{8}$$

The dilatation coefficient β was estimated using, as before, data extracted from dilatometry tests performed at very low ramp heating in order to ensure a mechanical and thermal equilibrium, so that $\sigma = 0$ and $\varepsilon = \varepsilon_v$, and hence:

$$\left.\frac{d\varepsilon}{d\theta}\right]_{\sigma=0,\varepsilon_v=\varepsilon} = \beta. \tag{9}$$

The K modulus was obtained using relaxation tests at different strain amplitudes. The K modulus is the slope of the straight line which describes the correspondence between the stress level and the strain amplitude once the mechanical and thermal equilibrium is reached.

$$\left.\frac{\sigma}{\varepsilon}\right]_{\varepsilon_v=\varepsilon,\theta=0} = K\,. \tag{10}$$

3. Analysis of thermoelastic effects of PMMA and PC polymers

These materials are very often used in industrial applications. Both polymers were provided by ATOFINA. We used standard dog bone shaped test specimens with the following gauge part sizes: length (60 mm), width (10 mm), thickness (4 mm). The main thermophysical characteristics of both materials are grouped in Table 1. Note that the temperature T_β corresponding to the first sub-vitreous relaxation peak of the PMMA is slightly greater than the room temperature at which the tests were performed ($T_0 \approx$20-24°C), while the relaxation peak temperature of the PC polymer is highly negative. At around room temperature, the PC samples consequently showed greater molecular mobility than the PMMA samples. Due to this property, the PC samples had good ductility while the PMMA samples remained particularly brittle. As the glass transition temperature of both polymers is greater than 100°C, they naturally remained in a glassy state during the deformation tests. Besides, the α and β coefficients were measured under the same experimental conditions. Hence $\alpha=\beta$ even though a different thermodynamic path depending on the model is associated with a (very slow) dilatometry test (cf. Eqs (5) and (9)).

	ρ (measured) ($Kg.m^{-3}$)	C [8] ($J.Kg^{-1}.°C^{-1}$)	κ [8] ($W.m^{-1}.K^{-1}$)	$\alpha=\beta$ (measured) ($°C^{-1}$)	E (measured) (MPa)	K (measured) (MPa)	T_β [9] (°C)	T_g [9] (°C)
PMMA	1160	1450	0.17	70.10^{-6}	3650	3500	35	105-120
PC	1190	1200	0.2	70.10^{-6}	2650	2570	-70	145

Table 1. Thermophysical properties of PMMA and PC
Tableau 1. Propriétés thermophysiques du PMMA et du PC

Figures 2 and 4 show a time course presentation of the longitudinal temperature profiles $\theta(x,t)$ recorded by the infrared camera. In order to depict the θ profiles as a function of loading, the tensile stress was superimposed (black curve). When the regularity of the specimen geometry and the low material diffusivity were taken into account, we considered that the mean heat source over each cross-section was sufficiently representative of the material behaviour [6]. The uniform character of the temperature profiles is indeed consistent with a homogeneous distribution of the sources, especially for materials with low thermal diffusivity.

The primacy of the thermoelastic effects over the dissipation can easily be checked: Figures 2 and 4 indicate a distinct cooling of the specimen during the loading stages and heating during the unloading stages, with the mean temperature over each load-unload cycle being approximately zero. The image processing methods used to estimate heat source patterns have already been thoroughly described in [5]. A one-dimensional thermal diffusion model was used hereafter. Where *Oz* denotes the loading direction, the diffusion equation reads:

$$\rho C\left(\frac{\partial\theta}{\partial t}+\frac{\theta}{\tau_{th}}\right)-k\frac{\partial^2\theta}{\partial z^2}=w'_{ch}\,, \tag{11}$$

where τ_{th} is a time constant characterizing heat losses perpendicular to the loading direction, w'_{ch} is the overall heat source which here comes essentially from thermoelastic couplings. The time constant τ_{th} was estimated while considering the temperature variations in the middle of the sample gauge part during the return to thermal equilibrium [5]. Hence, $w'_{ch} \approx s^{\Theta}_{the}$, where s^{Θ}_{the} is the thermoelastic source derived from infrared data. In Figures 3 and 5, we plotted variations in s^{Θ}_{the}, i.e. the thermoelastic source derived from the PT type model s^{PT}_{the} and from the Zener type model s^{Z}_{the}. These

two latter sources were computed using stress and strain measurements: $s_{\text{the}}^{\text{PT}} \approx -\alpha T_0 \dot{\sigma}$ ($E\alpha^2 T_0 / \rho C < 4‰$), and $s_{\text{the}}^{\text{Z}} = -\beta T_0 K \dot{\varepsilon}$.

Concerning the PMMA behaviour, Figure 3 shows that the variations in s_{the}^{Θ} and $s_{\text{the}}^{\text{Z}}$ remained close at all the stress levels. Conversely, the source $s_{\text{the}}^{\text{PT}}$ was quasi linear throughout the loading while s_{the}^{Θ} remained almost constant. In Figure 5, the estimates of the three thermoelastic sources s_{the}^{Θ}, $s_{\text{the}}^{\text{Z}}$, $s_{\text{the}}^{\text{PT}}$ were plotted. Concerning the PC behaviour, a better prediction was obtained with the PT type model.

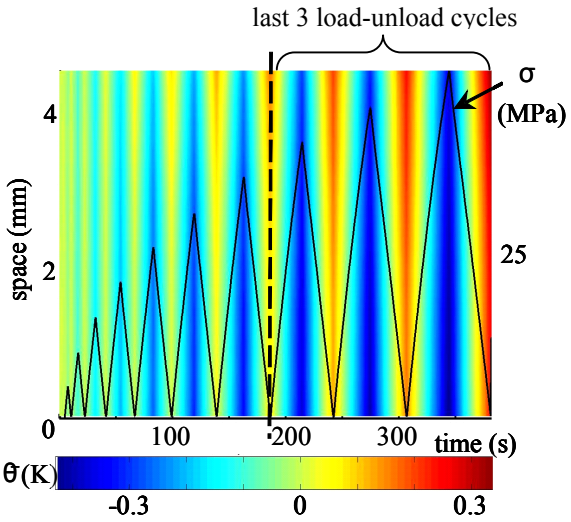

Fig.2: PMMA mechanical and thermal responses during a cyclic pulsating test.
Fig.2: Réponses mécanique et thermique du PMMA au cours d'un essai cyclé.

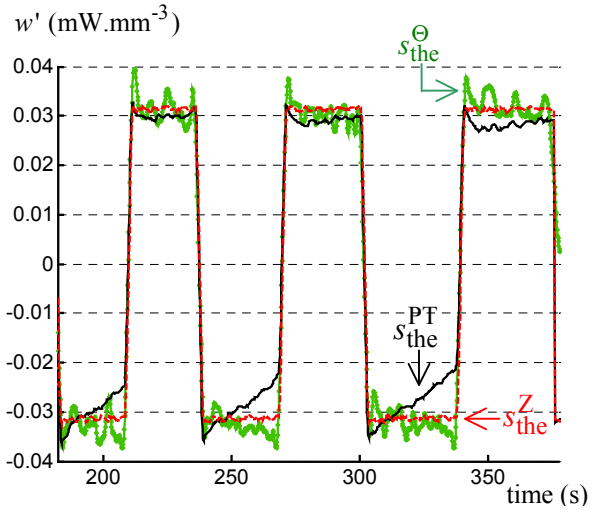

Fig.3: s_{the}^{Θ}, $s_{\text{the}}^{\text{Z}}$, $s_{\text{the}}^{\text{PT}}$ patterns associated with the last three load-unload cycles (PMMA).
Fig.3: Evolutions de s_{the}^{Θ}, $s_{\text{the}}^{\text{Z}}$ et $s_{\text{the}}^{\text{PT}}$ associées aux trois derniers cycles de charge-décharge, (PMMA).

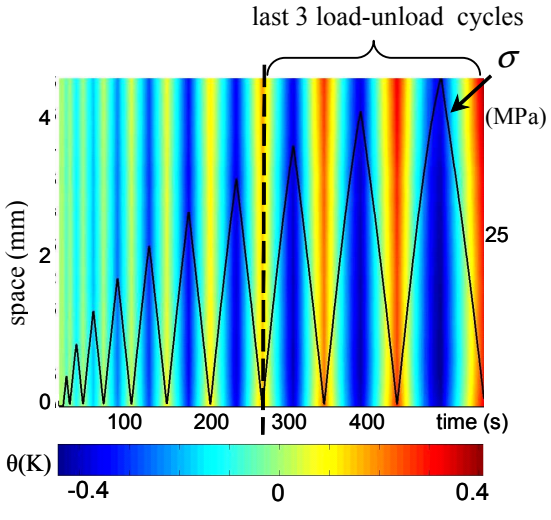

Fig.2b4: PC mechanical and thermal responses during cyclic pulsating tests.
Fig.4: Réponses mécanique et thermique du PC au cours d'un essai cyclé.

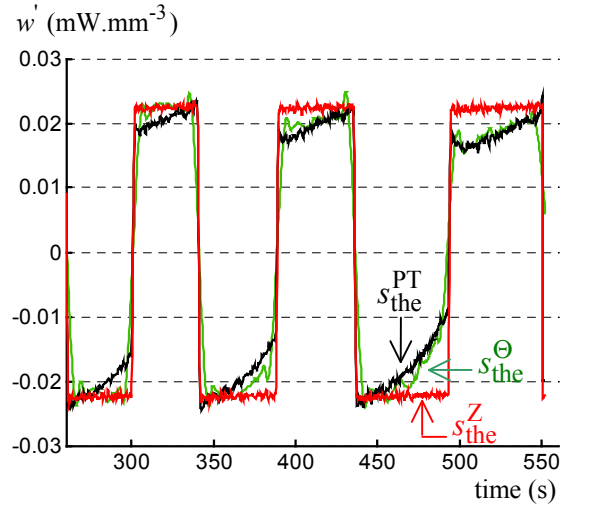

Fig.5: s_{the}^{Θ}, $s_{\text{the}}^{\text{Z}}$, $s_{\text{the}}^{\text{PT}}$ patterns associated with the last three load-unload cycles, (PC).
Fig.5: Evolutions de s_{the}^{Θ}, $s_{\text{the}}^{\text{Z}}$ et $s_{\text{the}}^{\text{PT}}$ associées aux trois derniers cycles de charge-décharge, (PC).

For the two materials studied, it should be noted that the order of magnitude of the thermoelastic source amplitude was about 60 $\mu W.mm^{-3}$ whereas the dissipation intensity remained under 2 $\mu W.mm^{-3}$.

4. Concluding comments

Within a small perturbation framework, the results of thermographic experiments led us to use viscothermoelastic models to describe the thermomechanical behaviour of PMMA and PC polymers. Indeed, from an energy standpoint, we observed a predominance of thermoelastic effects as compared to viscous dissipation. In this context, we noted a non-systematic equivalence between "series" and "parallel" models. This distinction appeared to be useful for describing differences in thermoelastic effects on PMMA and PC behaviours under the same loading conditions. A comparison of the thermoelastic sources, first derived from thermal data and secondly computed with mechanical measurements, showed that PMMA resembles a Z type model while PC resembles a PT type model. Complementary analyses are currently under way to determine if this behavioural difference is correlated with the intensity of molecular mobility.

[1] M. A. Biot, *Mechanics of incremental deformations*, J. Wiley & Sons Eds., 1965, Chap. VI, pp. 337-396.
[2] J. D. Ferry, *Viscoelastic properties of polymers*, J. Wiley & Sons Eds, 1980, Chap. I, pp. 1-32.
[3] T.Alfrey,Jr., *Mechanical behaviour of high polymers*, Vol. VI, Chap. B, Interscience Publishers, INC, New-York, 1948, pp. 93-233.
[4] S. Moreau, *Etude calorimétrique par thermographie infrarouge de la thermo-visco-élasticité de quatre polymères*, PhD Thesis, Montpellier University, 2004.
[5] A. Chrysochoos, H. Louche, *An infrared image processing to analyse the calorific effects accompanying strain localisation*, International Journal Engineering Sciences, 38, (2000) pp 1759-1788.
[6] P. Germain, Q. S. Nguyen, P. Suquet, *Continuum thermodynamics*, Journal of Applied Mechanics, vol. 50, (1983) pp. 1010-1020.
[7] J. Lemaitre, J.-L. Chaboche, *Mechanics of Solid Materials*, Cambridge University Press, 1990, Chap.II, pp.37-68.
[8] Atofina, Documentation, http://www.atofina.com/groupe/fr/f_elf_2.cfm.
[9] G.W. Ehrenstein, F. Montagne, Matériaux polymères. Hermès Science Publications, 1999. pp 302-319.